Journal of Magnetic Resonance **143,** 417–422 (2000)
doi:10.1006/jmre.2000.2032, available online at http://www.idealibrary.com on IDEAL®

Simple Suppression of Spurious Peaks in TROSY Experiments

Chojiro Kojima and Masatsune Kainosho[1]

CREST, Japan Science and Technology Corporation, and Department of Chemistry, Faculty of Science, Tokyo Metropolitan University, 1-1 Minami-ohsawa, Hachioji, Tokyo, 192-0392 Japan

Received October 8, 1999; revised January 13, 2000

In ^{1}H–^{15}N TROSY experiments of proteins and nucleic acids, where the second coherence transfer delay time τ' has been fixed as 5.6 ms, $1/(2^{1}J_{NH})$, in order to achieve complete spin-state selection, spurious negative peaks are observed along the ^{15}N axes. These peaks are often annoyingly large, especially for nucleic acids. A simple product operator calculation, however, indicated that the shortening of the second delay time τ', which is next to the $t1$ period, would efficiently suppress these spurious peaks, without sacrificing the sensitivities of the TROSY peaks too much. We have shown for three systems, two 11- and 17-kDa proteins and one 8-kDa DNA duplex, that these spurious peaks can be effectively suppressed with delay times of 3.3 ms for the two proteins and 2.3 ms for the DNA. These delay times, optimized by trial and error, for the spurious peak suppression did not depend on the magnetic field strength and the temperature very much. Although the shortened τ' delay times attenuate the TROSY peak intensities by about 10 and 20% for the two proteins and the DNA, respectively, this simple modification will be useful for the quantitative uses of TROSY peaks and will result in cleaner spectra for various TROSY-based multiple resonance experiments.

Key Words: **^{1}H–^{15}N TROSY experiment; spurious peak suppression; isotopically labeled biomacromolecules; nucleic acids; protein.**

INTRODUCTION

Transverse relaxation optimized spectroscopy, TROSY, recently developed by Pervushin *et al.* (*1*), is an extremely important breakthrough in biological NMR techniques. TROSY experiments allow, for example, the detailed spectral analyses of proteins as large as 110 kDa (*2*), which are definitely too large to be handled by conventional NMR spectroscopy, and thus TROSY is quickly becoming an essential tool for NMR studies of larger biological macromolecules. The peak intensities of TROSY can be improved by a factor of $\sqrt{2}$ (*3–11*), with either a sensitivity enhancement scheme (*12*) or a gradient coherence selection scheme with sensitivity enhancement (*13*). With this sensitivity improvement, the integrated peak intensities of the TROSY spectra become half of those of the conventional HSQC spectra, although one of the four multiplet components of HSQC is actually detected in TROSY (*3–11*). If one takes the relaxation effects into consideration, then TROSY becomes very attractive and is 1.1 times more sensitive compared to HSQC for a 45-kDa protein (*3*). The much narrower linewidths in both dimensions make TROSY experiments important not only for large molecules but also for most experiments requiring narrower linewidths.

Although the TROSY experiment has a big advantage in its much narrower linewidths, there is a hidden spurious peak, which was pointed out by Rance *et al.* (*8*). For the ^{1}H–^{15}N TROSY, a negative peak in the ^{15}N dimension appears, due to the difference in the relaxation rates between single quantum ^{15}N magnetization and multiquantum ^{1}H–^{15}N magnetization. The spurious peak in the ^{15}N dimension is dominated by the chemical shift anisotropy (CSA) of the proton and proton–proton dipolar interactions with the remote protons. When the CSA term is dominant, the magnitude of the spurious peak depends on the magnetic field strength. On the other hand, when the ^{1}H–^{1}H dipolar interactions are dominant, the spurious peak is independent from the magnetic field strength. We examined the magnetic field strength dependence of the spurious peak and its elimination. The simple product operator calculation was used to find a way to eliminate the spurious peak, and the delay time next to the $t1$ period was found to be important. Experimentally, the spurious peaks in the TROSY spectra were eliminated in three systems, one DNA (8 kDa) and two proteins (11 and 17 kDa).

THEORY

The TROSY spectrum is characterized by the sum or the difference of the in-phase and antiphase doublet components with a 1 to 1 ratio. Experimentally this ratio is not 1 to 1, since the relaxation rate of the antiphase components is faster than that of the in-phase ones, and thus the spurious peak appears in the spectrum. Rance *et al.* (*8*) expressed these spurious peaks using the product operator formalism including the relaxation rates. For example, the real component of the $f1$ quadrature signal, σ_R, is shown as

[1] To whom correspondence should be addressed. Fax: +81 (426) 77-2544. E-mail: kainosho@nmr.chem.metro-u.ac.jp.

1090-7807/00 $35.00

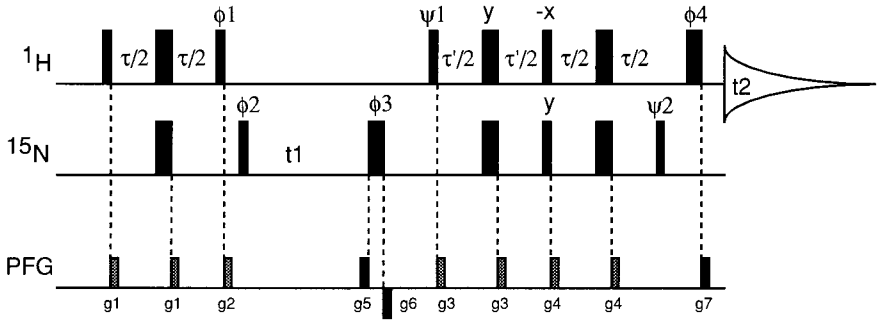

FIG. 1. Pulse sequence of the sensitivity- and gradient-enhanced TROSY. Thin and thick pulses are 90° and 180° pulses, respectively. Pulse phases are x unless indicated otherwise. P- and N-type signals are selected with sign inversions of PFGs g5/g6 and phases $\psi 1/\psi 2$. For the States–TPPI mode detection, sign inversion of the following is required: pulse phase $\phi 2$, receiver phase, and PFGs g5/g6. Phase cycle: $\phi 1 = 8(x), 8(-x)$; $\phi 2 = 4(x), 4(-x)$; $\phi 3 = 2(x), 2(-x)$; $\phi 4 = x, -x$; $\psi 1 = y$; $\psi 2 = x$; receiver $= 4(x), 8(-x), 4(x)$. Delay: $\tau = 1/(2^1J_{NH})$; $\tau' \leq 1/(2^1J_{NH})$. τ' is the delay time to be optimized for the spurious peak elimination.

$$\begin{aligned}\sigma_R = &-4I_y[\cos(\pi J_{NH}t_1)\cos(\Omega_N t_1)\exp(-[R_{MQ} + R_{2I}]\tau)\\ &- \sin(\pi J_{NH}t_1)\sin(\Omega_N t_1)\exp(-[R_{2S} + R_{2I}]\tau)]\\ &+ 8I_yS_z[\cos(\pi J_{NH}t_1)\cos(\Omega_N t_1)\exp(-2R_{MQ}\tau)\\ &- \sin(\pi J_{NH}t_1)\sin(\Omega_N t_1)\exp(-[R_{2S} + R_{MQ}]\tau)],\end{aligned} \quad [1]$$

where J_{NH} is the one-bond N–H scalar coupling constant, Ω_N is the chemical shift of the ^{15}N spin, and $\tau = 1/(2^1J_{NH})$. R_{2I}, R_{2S}, and R_{MQ} are the relaxation rate constants for ^{1}H single-quantum coherence, ^{15}N single-quantum coherence, and ^{1}H–^{15}N multiquantum coherence, respectively.

The exponential terms in Eq. [1] can be expanded to the first order in τ when the relaxation rates are assumed to be much less than $1/(4\tau) \sim 100\ s^{-1}$.

$$\begin{aligned}\sigma_R = &-4(I_y - 2I_yS_z)\cos[(\Omega_N + \pi J_{NH})t_1]\\ &\times [1 - (2R_{MQ} + R_{2I} + R_{2S})\tau/2] - 4(I_y - 2I_yS_z)\\ &\times \cos[(\Omega_N - \pi J_{NH})t_1](R_{2S} - R_{MQ})\tau/2\\ &- 4(I_y + 2I_yS_z)\cos[(\Omega_N + \pi J_{NH})t_1](R_{MQ} - R_{2I})\tau/2\end{aligned} \quad [2]$$

If $J(0) \gg J(\omega_I)$, then

$$\begin{aligned}\sigma_R = &-4(I_y - 2I_yS_z)\cos[(\Omega_N + \pi J_{NH})t_1]\\ &\times [1 - (2R_{MQ} + R_{2I} + R_{2S})\tau/2]\\ &- 4(I_y - 2I_yS_z)\cos[(\Omega_N - \pi J_{NH})t_1]\\ &\times 2J(0)\tau[d_{IS}^2/8 - c_I^2/6 - \Sigma_k d_{IK}^2/8]\\ &- 4(I_y + 2I_yS_z)\cos[(\Omega_N + \pi J_{NH})t_1]\\ &\times 2J(0)\tau[-d_{IS}^2/8 + c_S^2/6]\end{aligned} \quad [3]$$

and

$$d_{IS} = \gamma_I\gamma_S\hbar\mu_0 r_{IS}^{-3}/(8\pi^2) \quad [4]$$

$$c_I = \omega_I\Delta\sigma_I/3, \quad [5]$$

where $J(\omega)$ is the spectrum density function, μ_0 is the permittivity of free space, $\hbar$ is Planck's constant, γ is the gyromagnetic ratio, r_{IS} is the length of the IS bond, and $\Delta\sigma$ is the chemical shift anisotropy. The suffixes I, S, and K are related to the target amide or imino proton, the nitrogen, and the remote proton, respectively. All three rate constants contain contributions from remote protons, and the summations include all remote protons ($K \neq I$). In Eq. [3] the first, second, and third terms are the TROSY peaks at the frequency coordinates $(\Omega_N + \pi J_{NH}, \Omega_H - \pi J_{NH})$, $(\Omega_N - \pi J_{NH}, \Omega_H - \pi J_{NH})$, and $(\Omega_N + \pi J_{NH}, \Omega_H + \pi J_{NH})$, respectively. The first term is the target TROSY peak, and the other two are the spurious peaks. The amplitude of each peak is determined by the relaxation rates and the delay time τ. For example, when $R_{2S} \sim R_{MQ}$ and $R_{MQ} \sim R_{2I}$, no spurious peak will be generated. In general, the target peak is positive in-phase and $R_{MQ} \geq R_{2S}$, so the spurious peaks along the ^{15}N axis are negative.

In Fig. 1 the sensitivity- and gradient-enhanced TROSY pulse sequence is shown. For the case of $\tau' \neq \tau$, the amplitude of σ_R changes due to the relaxation. Assuming the relaxation rates are much less than $1/(4\tau')$ and $1/(4\tau) \sim 100\ s^{-1}$, and ignoring the imperfection of the spin-state selection, the relaxation effect may be described by the product operator formalism.

$$\begin{aligned}\sigma_R = &-4(I_y - 2I_yS_z)\cos[(\Omega_N + \pi J_{NH})t_1]\\ &\times [1 - (R_{MQ} + R_{2I})\tau/2 - (R_{MQ} + R_{2S})\tau'/2]\\ &- 4(I_y - 2I_yS_z)\cos[(\Omega_N - \pi J_{NH})t_1]\\ &\times (R_{2S} - R_{MQ})\tau'/2 - 4(I_y + 2I_yS_z)\\ &\times \cos[(\Omega_N + \pi J_{NH})t_1](R_{MQ} - R_{2I})\tau/2\end{aligned} \quad [6]$$

In comparison to Eq. [2] the TROSY peak intensities at the frequency coordinates, $(\Omega_N + \pi J_{NH}, \Omega_H - \pi J_{NH})$ and $(\Omega_N - \pi J_{NH}, \Omega_H - \pi J_{NH})$, the first and second terms, are different, but that of $(\Omega_N + \pi J_{NH}, \Omega_H + \pi J_{NH})$, the third term, is identical. The difference is characterized by a factor $[1 - (2R_{MQ} + R_{2I} + R_{2S})\tau/2]/[1 - (R_{MQ} + R_{2I})\tau/2 - (R_{MQ} + R_{2S})\tau'/2]$ and τ/τ' for the target and the spurious peaks along the ^{15}N axis, respectively. When $\tau' < \tau$, the intensities of the target and the spurious peaks increase and decrease, respectively, compared to that for $\tau' = \tau$. Note that when changing the delay time τ' the peak intensity is also changed, but the sign is not affected.

When $\tau' \neq \tau$, the spin-state selection does not work well and an artifact appears along the ^{15}N axis. Ignoring the relaxation effect, σ_R is written as

$$\begin{aligned}\sigma_R = &-4(I_y - 2I_yS_z)\cos[(\Omega_N + \pi J_{NH})t_1] \\ &\times [1 + \sin(\pi J_{NH}\tau')]/2 - 4(I_y - 2I_yS_z) \\ &\times \cos[(\Omega_N - \pi J_{NH})t_1][1 - \sin(\pi J_{NH}\tau')]/2. \quad [7]\end{aligned}$$

If $\tau' = 2n \times \tau$, where n is either zero or a positive integer, then the intensity of the artifact is positive and identical to that of the target peak. If $\tau' = (4n + 1) \times \tau$, no artifact peak is generated, and if $\tau' = (4n + 3) \times \tau$, no target peak is generated. Since the $\sin(\pi J_{NH}\tau')$ value changes from -1 to $+1$ when changing the delay time τ', the intensities of the target and the artifact peaks are controlled from zero to a positive, maximum value (see Eq. [7]). The real signal may be explained by the sum of two factors, the relaxation (Eq. [6]) and the imperfection of spin-state selection (Eq. [7]). Therefore, the optimal delay time τ' exists where the two factors cancel each other, the negative spurious peak caused by the relaxation effect and the positive artifact generated by the imperfection of the spin-state selection.

EXPERIMENTAL

Three ^{15}N-enriched samples, one DNA and two proteins, were used to examine and demonstrate the spurious peak elimination in TROSY. The double-stranded DNA sample, ca. 2 mM, contained 100 mM NaCl, 10 mM phosphate buffer, and 0.1 mM EDTA (pH 6.8). The sequence was the self-complement d(CGC**GA**AT**TC**GCG)$_2$, in which bold letters represent ^{15}N-labeled residues (12 bp, 8 kDa). The two protein samples were the uniformly ^{15}N-labeled cystatin A (97 aa, 11 kDa) (*14*) and the protein–protein complex of the ^{15}N-labeled Box A domain of the HMG1 protein (82 aa, 9.6 kDa) and the nonlabeled homeo domain of the HOX-D9 protein (61 aa, 7.8 kDa) (*15*). The concentration of the protein–protein complex sample was ca. 1 mM, including 100 mM KCl, 1mM DTT, 5% glycerol, and 0.02% NaN_3 (pH 5.5), and for cystatin A it was ca. 1 mM, including 10 mM sodium acetate buffer (pH 4.0). The volume of each sample was about 250 μl in a 5-mm Shigemi tube.

NMR experiments were performed on Bruker DRX600 and DRX800 spectrometers using a ^{1}H–^{13}C–^{15}N triple-resonance probe-head equipped with an *XYZ* triple-axis gradient. The TROSY pulse sequence is shown in Fig. 1. The delay time τ' was changed from 0 to 5.6 ms and was optimized to eliminate the spurious peaks along the ^{15}N axis. The following temperatures were examined: 2, 20, and 30°C on 600 MHz and 20°C on 800 MHz for DNA; 35°C on 600 MHz for cystatin A; and 20°C on 600 and 800 MHz for the HMG1–HOX-D9 complex. For the evaluation of the relative intensity of the spurious peak, the ^{15}N 1D slice was obtained by calculating the sum of the 1D slices over the peak range in the ^{1}H dimension with XWIN-NMR software (Bruker). The product operator calculation was performed using POMA (*16*) on Mathematica software (Wolfram Research, Inc.).

RESULTS AND DISCUSSION

Rance *et al.* demonstrated that two types of spurious peaks are observed in TROSY (*8*). One was the large spurious peak along the ^{15}N axis, and the other was small and along the ^{1}H axis. Comparing these two spurious peaks, the difference in their magnitudes was more than 10-fold, and the relative intensity of the small spurious peak was about 1% of the target peak. The peak shape of the latter spurious peak was not due only to absorption, and the sign judgement was also difficult. This meant that the expression of Eqs. [2, 3] was not exact for this small spurious peak. Thus, we focused on the former large spurious peak and did not consider the latter. For the large spurious peaks, two origins, as shown in Eq. [3], were considered: the proton CSA term and the dipolar term between the target and the remote protons (*8*). To see which is important, the magnetic field strength dependence was examined using 600- and 800-MHz spectrometers. For the DNA, the relative intensity of the spurious peak was 25 $\sim$ 40% increased on 800 MHz compared to 600 MHz, but for the proteins the intensity was similar or less. This result was self-conflicting, but may suggest the presence of some exchange terms for the DNA and the insignificance of the proton CSA term for the proteins.

By changing the delay time τ' (see Fig. 1), the spurious peak along the ^{15}N axis could be eliminated, as described under Theory (see Eqs. [6] and [7]). In Fig. 2, the ^{15}N 1D slices of the sensitivity- and gradient-enhanced ^{1}H–^{15}N TROSY spectra of DNA are presented. The top spectrum was recorded with $\tau' = \tau = 5.6$ ms, and the bottom was with $\tau' = 2.3$ ms. In the bottom spectrum, the spurious peak along the ^{15}N axis was completely eliminated. The delay time τ' was optimized by changing the delay time τ', as shown in Fig. 3. The open circles and the cross points were the relative peak intensities of the spurious peaks for the guanosine and thymine imino groups, respectively, which were measured at three different temperatures, 2, 20, and 30°C, on a 600-MHz spectrometer. The solid

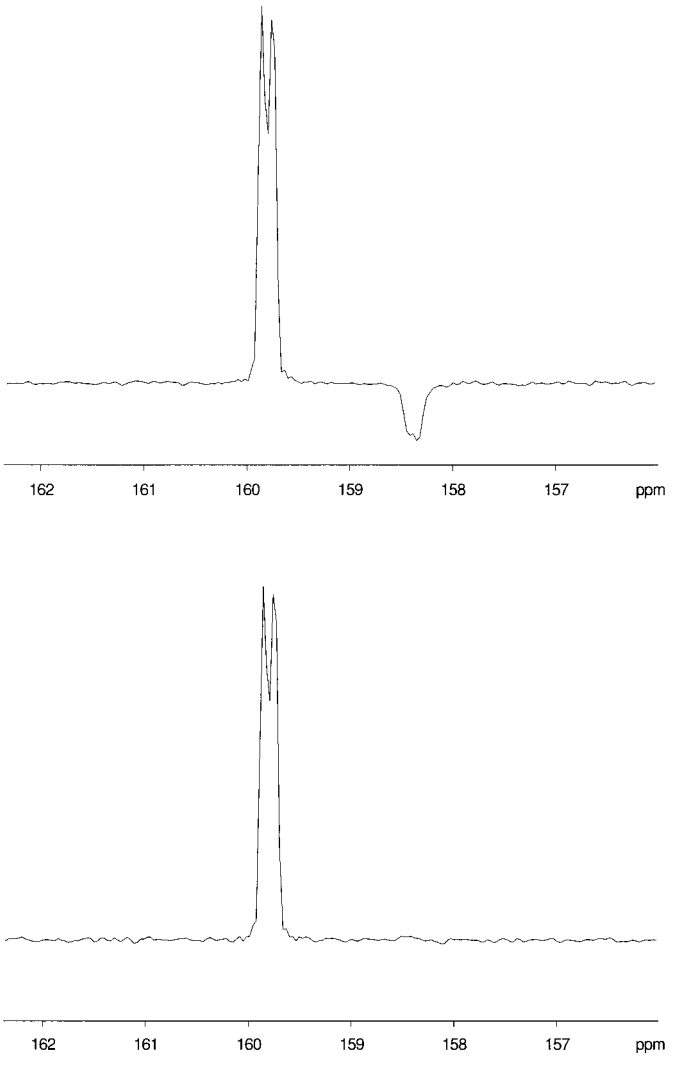

FIG. 2. 1D slices of the thymine imino ^{15}N from TROSY spectra of 8-kDa DNA measured at 20°C on 600 MHz. (Top) Conventional and (bottom) the spurious peak eliminated spectra, $\tau' = 5.6$ ms and 2.3 ms, respectively. The pulse sequence of Fig. 1 is used.

curve was calculated from the ratio, $[1 - \sin(\pi J_{NH}\tau')]/[1 + \sin(\pi J_{NH}\tau')]$, which is the intensity ratio of the spurious peak to the target, as shown in Eq. [7]. The dotted curves were obtained by smoothing the observed values for each guanosine and thymine at three temperatures. The solid and dotted curves were similar to each other, but did not fit well by adding or subtracting a constant value. Such differences may be due to the relaxation of the spurious peak itself.

The effects of the length of the delay time τ and the ^{1}H and ^{15}N flip angles on TROSY were also examined by the simple product operator calculation. By changing the ^{1}H and ^{15}N pulse lengths and the delay time τ, all of the magnetizations were attenuated, but the relative intensities of the four components were not altered and it was not useful to eliminate the spurious peaks. The imperfection of the ^{1}H pulse length caused mixing of the real and imaginary parts during $t1$. It was also not useful for eliminating the spurious peaks. These calculated results were experimentally confirmed by changing the delay time τ and the ^{1}H and ^{15}N pulse lengths. The absolute power of the gradients did not affect the relative intensities of the spurious peaks.

The spurious peak elimination technique used for the TROSY spectrum of the DNA was also applicable to the proteins. In Fig. 4, four spectra are shown to demonstrate how well our procedure worked for the 11- and 17-kDa proteins. The left two spectra are for the 11-kDa protein, and the right two are for the 17-kDa protein–protein complex. The top spectra were measured by the conventional TROSY parameters and the lower spectra were by the optimal values, $\tau' = 3.3$ ms. Our procedure for the spurious peak elimination did work well in the limited narrow spectral region, as shown in Fig. 4. However, the optimal τ' value was slightly different depending on the proton chemical shift, and thus there was no optimal value that eliminated all of the spurious peaks over the entire spectrum. This was because the amide and imino proton CSA values depended on the isotropic chemical shift value (*17*), and that CSA value changed the amplitude of the spurious peak (see Eq. [3]). Moreover, theoretically the spurious peaks along the ^{1}H axis were not suppressed at all by our procedure, although this spurious peak was negligible, about 1% of the main signal.

The difference between the optimized τ' values for the protein (3.3 ms) and the DNA (2.3 ms) is too big to neglect. Since the optimal delay time τ' depends on both the proton CSA value and the strength of the proton–proton dipolar interaction, the observed difference in the τ' value between the DNA and the protein should be explained by the overall correlation time, the proton CSA values, and the proton density around the target proton. In Eq. [3] if the relation $\tau_i \ll \tau_o$ is

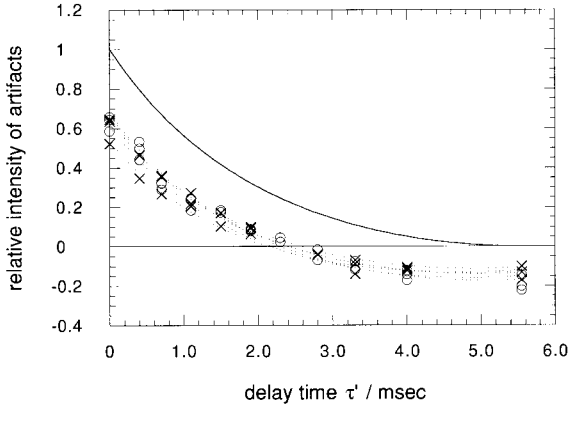

FIG. 3. Plots of the relative intensity of the spurious peak against delay time τ' measured at three different temperatures, 2, 20, and 30°C, on 600 MHz. The experimental conditions are identical to those of Fig. 2. The open circles and the cross points are the guanosine and thymine imino groups, respectively. The solid curve was theoretically calculated from Eq. [7]. The dotted curves were smoothed for the observed values.

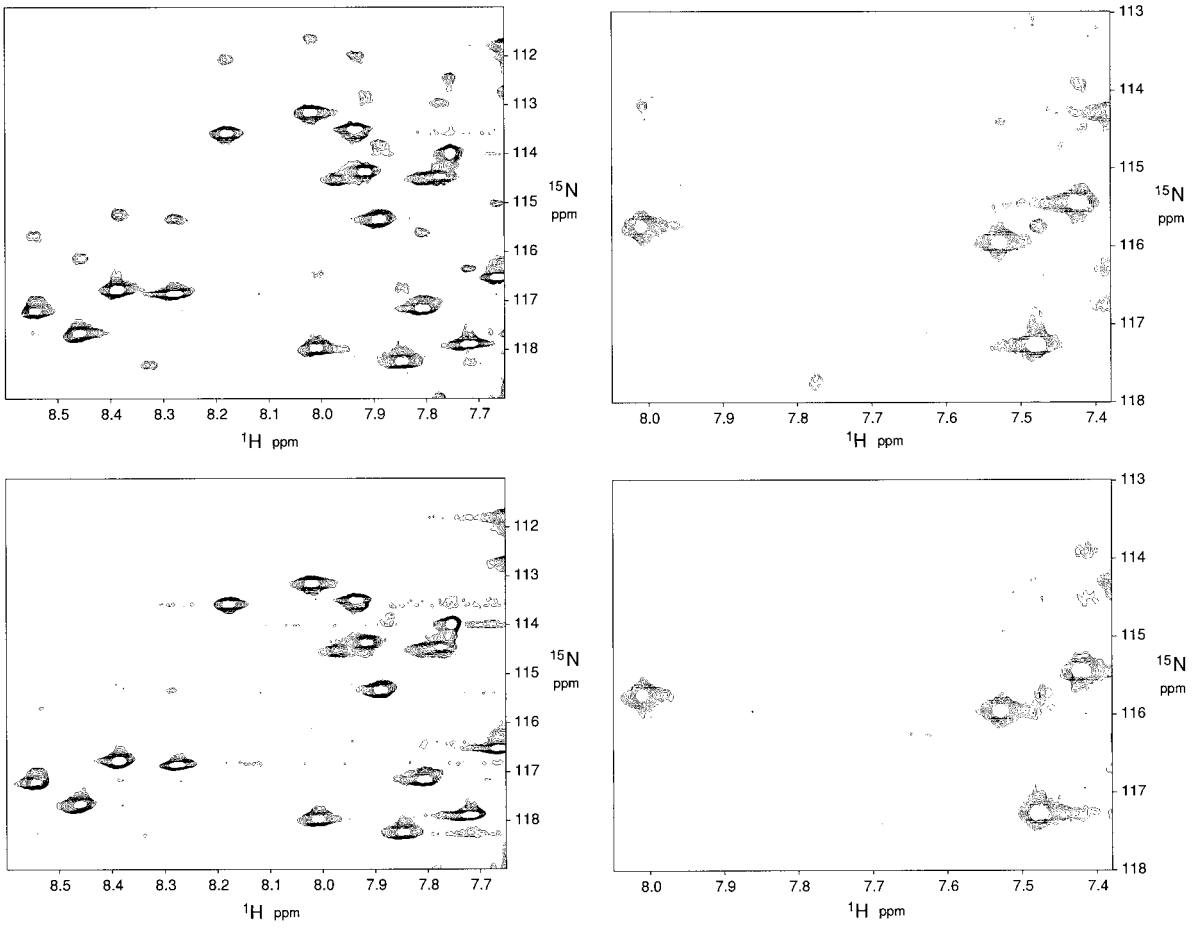

FIG. 4. (Left) A portion of the TROSY spectra for the 11-kDa protein cystatin A at 37°C on 600 MHz; (right) the TROSY spectra for the 17-kDa protein–protein complex at 20°C on 600 MHz. (Top) Conventional and (bottom) the spurious peak eliminated spectra, $\tau' = 5.6$ ms and 3.3 ms, respectively. The pulse sequence of Fig. 1 is used.

assumed, then we get the simple equation, $J(0) \approx S^2 \times \tau_o$, where τ_o and τ_i are the correlation times for overall and internal motion, and S^2 is the generalized squared order parameter. The magnitude of the spurious peaks along the ^{15}N axis is proportional to $2\tau[d_{IS}^2/8 - c_I^2/6 - \Sigma_k d_{IK}^2/8] \times S^2\tau_o$. The S^2 for the DNA imino NH group is about 0.8 (Kojima *et al.*, unpublished results) and that for the protein amide is $0.8 \sim 0.9$ or more. The overall correlation time τ_o is roughly proportional to the molecular weight. The proton density around the DNA imino proton is quite low compared to that for the amide proton. Considering these three factors, the spurious peak for our DNA (8 kDa) should be weaker than that for our protein (11 and 17 kDa), but this conflicts with our observed results. The residual factor is the proton CSA value. The exact CSA values for the imino and the amide protons are not known, but they do not seem to be very different. There is one thing we have not considered: the proton line broadening due to fast exchange with the bulk water. It affects the apparent relaxation rates, and in fact it is important for the DNA imino protons, since the exchange rate is faster than that for the proteins. The spurious peaks along the ^{15}N axis are proportional to $(R_{2S} - R_{MQ})\tau/2$, as shown in Eq. [2], and the R_{MQ} and R_{2I} terms include such a proton exchange term, but the R_{2S} term does not. If the proton exchange term is significantly large, then the spurious peaks increase and suppress other factors. This is one of the most reasonable explanations for our observation, and it is consistent with the observed magnetic field dependence, but additional experiments will be needed to prove it.

There are two other approaches to attenuate and eliminate the spurious peaks. One is deuterium labeling, where the proton–proton dipolar term is attenuated (*8*). The other procedure is the IPAP method (*18*), where the in-phase and the antiphase signals are recorded separately and summed or subtracted to get the single component in the ^{15}N dimension for the $^1J_{NH}$ measurement. Since the relaxation rates of each in-phase and antiphase component are not identical, the relative ratio of the two components for the summation and the subtraction cannot be equal to 1 to generate a pure, single component. The S/N ratio of IPAP is not very different from ours, but it is slightly worse due to the relaxation during the delay time $(\tau - \tau')$. The period from the first pulse to the detection in our experiment is shorter than that in IPAP, but our procedure requires several

experiments to optimize the delay time. The total experimental time of IPAP is clearly shorter than ours to obtain a pure, single component spectrum. Thus our procedure, involving shortening the delay time τ', should be understood as a simple procedure to attenuate the spurious peak for a system in which the optimal delay time is known from other proteins and nucleic acids.

The concept, shortening the delay time for the spurious peak elimination, seems to be generally applicable to spin-state selection experiments. For example, Meissner *et al*. have demonstrated that the spurious peaks due to relaxation cross-talk are eliminated by shortening a certain delay time (*19*). In their case, the spurious peak is positive instead of negative, and the procedure for the spurious peak elimination is slightly different from ours. It is important to note that our procedure will work with any triple-resonance experiment and any pulse sequence where TROSY is used.

CONCLUSION

The large negative spurious peaks along the ^{15}N axis in the ^{1}H–^{15}N TROSY spectra for proteins and nucleic acids were investigated by changing the temperature, the magnetic field strength, and the pulse parameters. Shortening the delay time τ' next to the $t1$ period was used to suppress the spurious peaks in the TROSY spectra of three samples, an 8-kDa DNA duplex and two proteins (11 and 17 kDa). For complete spurious peak suppression, the delay time τ' was optimized to be 2.3 ms for the DNA duplex and 3.3 ms for the two proteins, which had fixed delay times of 5.6 ms $= 1/(2^{1}J_{NH})$ for the complete spin-state selection. The optimized τ' delay times, 2.3 and 3.3 ms for the DNA and the two proteins, respectively, did not depend on the temperature and the magnetic field strength very much. Shortening the delay time τ' in Fig. 1 will work with any TROSY-based experiment as a simple tool to suppress the spurious peaks.

ACKNOWLEDGMENTS

We thank Drs. Akira Ono, Shin-ichi Tate, and Shinya Ohki for the labeled samples and Dr. Konstantine Pervushin for mentioning Ref. (*8*). This work was supported by CREST (Core Research for Evolutional Science and Technology) of the Japan Science and Technology Cooperation (JST) and by a Grant-in-Aid for Scientific Research on Priority Areas from the Ministry of Education, Science, and Culture (09235237).

REFERENCES

1. K. Pervushin, R. Riek, G. Wider, and K. Wüthrich, *Proc. Natl. Acad. Sci. USA* **94,** 12366–12371 (1997).
2. K. Wüthrich, *Nat. Struct. Biol.* **5,** 492–495 (1998).
3. P. Andersson, A. Annila, and G. Otting, *J. Magn. Reson.* **133,** 364–367 (1998).
4. B. Brutscher, J. Boisbouvier, A. Pardi, D. Marion, and J.-P. Simorre, *J. Am. Chem. Soc.* **120,** 11845–11851 (1998).
5. M. Czisch and R. Boelens, *J. Magn. Reson.* **134,** 158–160 (1998).
6. A. Meissner, T. Schulte-Herbrüggen, J. Briand, and O. W. Sørensen, *Mol. Phys.* **95,** 1137–1142 (1998).
7. K. Pervushin, G. Wider, and K. Wüthrich, *J. Biomol. NMR* **12,** 345–348 (1998).
8. M. Rance, J. P. Loria, and A. G. Palmer, III, *J. Magn. Reson.* **136,** 92–101 (1999).
9. J. Weigelt, *J. Am. Chem. Soc.* **120,** 10778–10779 (1998).
10. G. Zhu, X. M. Kong, X. Z. Yan, and K. H. Sze, *Angew. Chem. Int. Ed.* **37,** 2859–2861 (1998).
11. G. Zhu, X. M. Kong, and K. H. Sze, *J. Biomol. NMR* **13,** 77–81 (1999).
12. J. Cavanagh, A. G. Palmer, III, P. E. Wright, and M. Rance, *J. Magn. Reson.* **91,** 429–436 (1991).
13. L. E. Kay, P. Keifer, and T. Saarinen, *J. Am. Chem. Soc.* **114,** 10663–10665 (1992).
14. S. Tate, T. Ushioda, N. Utsunomiya-Tate, K. Shibuya, Y. Ohyama, Y. Nakano, H. Kaji, F. Inagaki, T. Samejima, and M. Kainosho, *Biochemistry* **34,** 14637–14648 (1995).
15. V. Zappavigna, L. Falciola, M. H. Citterich, F. Mavilio, and M. E. Bianchi, *EMBO J.* **15,** 4981–4991 (1996).
16. P. Güntert, N. Schaefer, G. Otting, and K. Wüthrich, *J. Magn. Reson. A* **101,** 103–105 (1993).
17. N. Tjandra and A. Bax, *J. Am. Chem. Soc.* **119,** 8076–8082 (1997).
18. M. Ottiger, F. Delaglio, and A. Bax, *J. Magn. Reson.* **131,** 373–378 (1998).
19. A. Meissner, T. Schulte-Herbrüggen, and O. W. Sørensen, *J. Am. Chem. Soc.* **120,** 7989–7990 (1998).